

## CHAPTER II

### LITERATURE REVIEW

#### 2.1 THEORETICAL BACKGROUND

##### 2.1.1 Theory of Gas Transport in Membranes

Membrane separation technology remains attractive opportunities for many industries due to several reasons. Firstly, the membrane is a simple separation method and involves no moving parts lead to using less energy for operation. Secondly, this technology is generally carried out at atmospheric conditions which can be important for sensitive applications. Thirdly, membrane separation is a continuous process, making membrane modules a more attractive option for plant retrofitting. Finally, the membrane separation takes advantage not only of differences in solubility of the chemicals to be separated but also of differences in diffusivity, thereby potentially achieving higher selectivity for a given separation (Li *et al.*, 2011).

At the current stage of development, the main cost is the energy required to create a large enough pressure difference across the membrane to drive separation. A membrane acts as a semi-permeable barrier. In general, the rate at which a particular gas will move through the membrane can be determined by the size of the molecule, the concentration of gas, the pressure difference across the membrane, and the affinity of the gas for the membrane material. There are a number of mechanisms for gas separation in membranes (Leiknes, 1999):

(1) Knudsen diffusion: the gas components are separated based on the difference in the mean path of the gas molecules.

(2) Molecular sieving: the gas components are separated based on size exclusion, the size being the kinetic diameter of the gas molecules.

(3) Solution-diffusion: the gases are separated by their solubility within the membrane and their diffusions through the dense membrane matrix. This is the usual separation mechanism for polymeric membranes (rubbers, polyimides, cellulose acetate).

(4) Surface diffusion: the gas molecules with higher polarity are selectively adsorbed onto the surface of the membrane and pass through the membrane by moving from one adsorption site to another side.

(5) Capillary condensation.

However, the most common mechanism is molecular sieving and solution-diffusion which are occurring in the polymeric membranes.

### 2.1.2 Polymeric Membranes

A polymeric membrane is widely used due to its relatively easy to manufacture and it is suitable for low temperature applications. There are three types of the polymeric membrane based on mechanism of gas separation. First, porous membrane uses molecular sieve to separate one type of molecules from other molecules by using diffusion mechanism. While passing through porous membrane with gases, the smaller molecule can diffuse into pores of membrane and pass through a permeate side. For bigger molecules, they can diffuse down into pores of membrane and cannot pass through permeate side, but they are rejected and stay at retentate side of the membrane. The molecular sieving mechanism is shown in Figure 2.1.

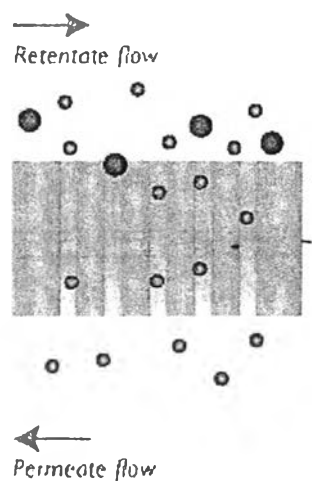


**Figure 2.1** The molecular sieving mechanism for porous membrane ([www.co2crc.com.au/aboutccs/cap\\_membranes.html](http://www.co2crc.com.au/aboutccs/cap_membranes.html)).

The second type of the polymeric membrane is nonporous membrane or dense membrane by using the difference in solution-diffusion of molecule. There are three steps in solution-diffusion mechanism for dense membrane: (1) adsorption or absorption upon the upstream boundary, (2) diffusion through the polymeric membrane, and (3) desorption or dissolution at the opposite interface of the membrane. This solution-diffusion mechanism is driven by a difference in thermodynamic activity between the interface of upstream and downstream. The solution-diffusion mechanism is shown in Figure 2.2.

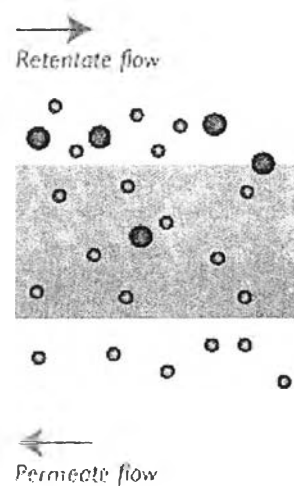


**Figure 2.2** The solution-diffusion mechanism for nonporous membrane ([www.co2crc.com.au/aboutccs/cap\\_membranes.html](http://www.co2crc.com.au/aboutccs/cap_membranes.html)).

The third type is called an asymmetric membrane. Asymmetric membrane denotes the structure consisting of a dense skin layer and a porous support layer. In the support layer, the polymer matrix and the pores are co-continuously connected across the layer. The three-dimensionally continuous polymer network exhibits the sufficient mechanical strength and allows gases to pass through the three-dimensionally continuous pores without gas resistance.

In polymeric membrane, the separation is based on a solution-diffusion mechanism, which involves molecular-scale interactions of the permeating molecule with the membrane polymer. The mechanism assumes that each molecule of gas is adsorbed by the membrane at one interface, transported by diffusion across the membrane through the voids between the polymeric chains (or called free

volume), and desorbed at the other interface. According to the solution-diffusion model, the permeation of molecules through membrane is controlled by two major parameters: the thermodynamic factors, called the solubility coefficient ( $S$ ) and a kinetic parameter, called the diffusivity coefficient ( $D$ ). Diffusivity is a measure of the mobility of individual molecules passing through the void between polymeric chains in a membrane material. The solubility coefficient equals the ratio of sorption uptake normalized by some measure of uptake potential, such as partial pressure. Solubility coefficient ( $S$ ) reflects the number of molecules dissolved in membrane material. Flux or permeability ( $P$ ) defined in Eq. (2.1), represents the quantity of mass transport through the membrane.

$$P = D \times S \quad (2.1)$$

where the permeability ( $P$ ) is in Barrer ( $1 \text{ Barrer} = 10^{-10} \text{ cm}^3 \cdot (\text{STP}) \cdot \text{cm} / (\text{cm}^2 \cdot \text{s} \cdot \text{cm} \cdot \text{Hg}) = 3.34 \times 10^{-16} \text{ mol} \cdot \text{m} / (\text{m}^2 \cdot \text{s} \cdot \text{Pa})$ ), the solubility ( $S$ ) is in  $\text{cm}^3 \cdot (\text{STP}) / (\text{cm}^3 \cdot \text{bar})$  and the diffusivity coefficient ( $D$ ) is in  $\text{cm}^2/\text{s}$ .

The ability of a membrane to separate two gas molecules called membrane selectivity,  $\alpha_{A/B}$  which is an ideal separation factor, can describe the ability of a membrane to separate gaseous mixture of  $A$  and  $B$  and can written as a ratio of the permeability of component  $A$  and  $B$ .

$$\alpha_{A/B} = \frac{P_A}{P_B} \quad (2.2)$$

where  $P_A$  and  $P_B$  are the permeabilities of pure gas  $A$  and  $B$  that pass through the membrane, respectively.

Since permeability depend on both diffusion coefficient ( $D$ ) which defected the mobility of each molecule in dense membrane, and solubility coefficient ( $S$ ) which reflected the number of molecules dissolved in membrane material, so membrane selectivity ( $\alpha_{A/B}$ ) can be written as product of the diffusivity selectivity and solubility selectivity.

$$\alpha_{A/B} = \left( \frac{D_A}{D_B} \right) \left( \frac{S_A}{S_B} \right) \quad (2.3)$$

where  $D_A/D_B$  is the diffusivity selectivity and  $S_A/S_B$  is the solubility selectivity.

The diffusivity selectivity is based on the inherent ability of polymer matrix to function as size and shape selectivity media. This ability is determined by such factor as polymer segmental mobility and intersegmental packing. The solubility selectivity, on the other hand, is determined by the difference of the condensabilities of the two penetrants as well as physical interaction of the penetrants with the particular polymer of which the membrane is composed.

### 2.1.3 Mixed Matrix Membranes (MMMs)

Mixed matrix membranes are a well-known route to enhance the properties of polymeric membranes. Their microstructure consists of an inorganic material in the form of micro- or nano-particles (dispersed phase) incorporated into a polymeric matrix (continuous phase). The use of two materials with different flux and selectivity provides the possibility to better design a membrane for CO<sub>2</sub> capture, allowing the synergistic combination of polymers easy processability and superior gas separation performance of inorganic materials. Furthermore the addition of inorganic materials in a polymer matrix offers enhanced physical, thermal and mechanical properties for aggressive environments and represents a way to stabilize the polymer membrane against change in permselectivity with temperature.

Permeation models for mixed matrix membranes with porous particles are used to predict effective permeability of a gaseous penetrant in a mixed matrix membrane as functions of continuous phase (polymer matrix) permeability, dispersed phase (porous particles) permeability and volume fraction of dispersed phase.

Bouma *et al.* (1997) used Maxwell–Wagner–Sillar model to calculate the effective permeability of a mixed matrix membrane with a dilute dispersion of ellipsoids:

$$P_M = P_c \left[ \frac{nP_d + (1-n)P_c - (1-n)\phi_d(P_c - P_d)}{nP_d + (1-n)P_c + n\phi_d(P_c - P_d)} \right] \quad (2.4)$$

where  $P_M$  is the effective permeability of a gaseous penetrant in a mixed matrix membrane,  $P_c$  is the continuous phase permeability,  $P_d$  is the dispersed phase permeability,  $\phi_d$  is the volume fraction of dispersed phase and  $n$  is the particle shape factor.

In this equation, the limit of  $n = 0$  leads to parallel two-layer model and can be expressed as an arithmetic mean of the dispersed and continuous phase permeabilities (Vu *et al.*, 2003 and Moore *et al.*, 2004):

$$P_M = \phi_d P_d + (1 - \phi_d) P_c \quad (2.5)$$

Moreover, when  $n = 1$  the Maxwell's model is simplified to a series two-layer model:

$$\frac{1}{P_M} = \frac{\phi_d}{P_d} + \frac{\phi_c}{P_c} \quad (2.6)$$

where  $\phi_c = (1 - \phi_d)$ .

It is very important to mention that the minimum and maximum values of the effective permeability of a penetrant in a mixed matrix membrane can be given by the series and parallel two-layer models, respectively. The minimum value corresponds to a series model and the maximum value of  $P_M$  occurs when both phases are assumed to work in parallel to the flow direction (Gonzo *et al.*, 2006).

Under the random particle distribution condition, one can use the geometric mean model to calculate effective permeability of a gas penetrant in a mixed matrix membranes:

$$P_M = P_c^{\phi_c} + P_d^{\phi_d} \quad (2.7)$$

In Eq. (2.4), then  $n = 1/3$  corresponds to dilute suspension of spherical particles and leads to the following equation known as the Maxwell's Equation:

$$P_M = P_c \left[ \frac{P_d + 2P_c - 2\phi_d(P_c - P_d)}{P_d + 2P_c + \phi_d(P_c - P_d)} \right] \quad (2.8)$$

Maxwell's model is the most famous equation to predict the mixed matrix membrane permeability. Maxwell presented this equation in 1873, to predict the electrical conduction through a heterogeneous media. On the other hand, because the electrical conduction through a heterogeneous media is analogous with the flux through membranes, one can use Maxwell's model to predict permeability in the mixed matrix membranes (Bouma *et al.*, 1997). This well-known equation has been used by several researchers to calculate mixed matrix membrane permeability.

The Maxwell's equation is applicable to a dilute suspension of spheres and can only be applicable for low loadings, when the volume fraction of filler particles is less than about 20%, because of the assumption that the streamlines around particles are not affected by the presence of nearby particles. In addition, the Maxwell model cannot predict the permeability of mixed matrix membranes at the maximum packing volume fraction of filler particles. Furthermore, the Maxwell model does not account for particle size distribution, particle shape, and aggregation of particles.

To calculate the permeability of mixed matrix membrane with a high filler volume fraction, the so-called Bruggeman model, originally developed for the dielectric constant of particulate composites, can be used. This equation considers the effect of adding additional particles to a dilute suspension and for random dispersion of spherical particles, which leads to:

$$\left(\frac{P_M}{P_c}\right)^{-1/3} \left(\frac{(P_M/P_c) - (P_d/P_c)}{1 - (P_d/P_c)}\right) = 1 - \phi_d \quad (2.9)$$

Although Bruggeman model is applicable for high loadings, this equation, similar to that of the Maxwell model, cannot predict the permeability of mixed matrix membranes at the maximum packing volume fraction of filler particles. In addition, it does not account for particle size distribution, particle shape, and aggregation of particles. Furthermore, to estimate effective permeability by using this equation, a trial and error procedure is needed.

The Lewis–Nielsen model, originally proposed for the elastic modulus of particulate composites, can be adapted to permeability as (Lewis *et al.*, 1997 and Nielsen, 1973):

$$P_M = P_c \left[ \frac{1 + 2(((P_d / P_c) - 1) / ((P_d / P_c) + 2))\phi_d}{1 - (((P_d / P_c) - 1) / ((P_d / P_c) + 2))\phi_d\psi} \right] \quad (2.10)$$

where  $\psi = 1 + \left( \frac{1 - \phi_m}{\phi_m^2} \right) \phi_d$  and  $\phi_m$  is the maximum packing volume fraction of filler particles, which is 0.64 for random close packing of uniform spheres.

The Lewis–Nielsen model may include the effects of morphology on permeability, because  $\phi_m$  is functions of particle size distribution, particle shape, and aggregation of particles.

Similar to the Lewis–Nielsen model, the Pal model can also be used to calculate the effective permeability of mixed matrix membranes with maximum packing volume fraction of filler particles and may include the effects of morphology on permeability through the parameter  $\phi_m$ . This equation is:

$$\left( \frac{P_M}{P_c} \right)^{1/3} \left( \frac{(P_d / P_c) - 1}{(P_d / P_c) - (P_M / P_c)} \right) = \left( 1 - \frac{\phi}{\phi_m} \right)^{-\phi_m} \quad (2.11)$$

However, the Pal model, like the Bruggeman model, is an implicit relationship that needs to solve numerically for  $P_M$ . On the other hand, according to the percolation theory, a simple power law can describe the relation between composite permeability and filler concentration near the percolation threshold (Gonzo *et al.*, 2006):

$$P_M = P_c (\phi_d - \phi_t)^t \quad (2.12)$$

where  $\phi_t$  is the percolation threshold (critical volume fraction of the filler) and  $t$  is the critical exponent.

Based on this theory, Chiew and Glandt (1983) presented an extension of Maxwell model in terms of  $\phi_d$ :



$$\frac{P_M}{P_c} \approx 1 + 3\beta\phi_d + 3(\beta\phi_d)^2 + O(\phi_d^3) \quad (2.13)$$

$$\beta \text{ is defined as: } \beta = \frac{P_d - P_c}{P_d + 2P_c}$$

where  $\beta$  is a convenient measure of penetrant permeability difference between the two phases and it is bounded by  $-0.5 \leq \beta \leq 1$ . Also,  $\beta = -0.5$  corresponds to totally non-permeable particle (e.g.  $P_d = 0.29$ ) and  $\beta = 1$  implies the perfectly permeable filler particle (disperse phase or  $P_c = 0$ ), while,  $\beta = 0$ , states the equal permeability in both phases.

In Eq. (2.13), the second term represents the interaction between particles and continuous media and the third term implies the interaction between particles.

In addition, by taking the original Maxwell equation, Chiew and Glandt proposed an equation in terms of  $\phi_d$  as below:

$$\frac{P_M}{P_c} = 1 + 3\beta\phi_d + K(\phi_d)^2 + O(\phi_d^3) \quad (2.14)$$

where  $K = a + b\phi_d^{1.5}$  and

$$a = -0.002254 - 0.123112\beta + 2.93656\beta^2 + 1.690\beta^3$$

$$b = 0.0039298 - 0.803494\beta - 2.16207\beta^2 + 6.48296\beta^3 + 5.27196\beta^4$$

It is obvious that when particle loading is low ( $\phi_d \ll 1$ ), term of order  $\phi_d^2$  and above is negligible in comparison with term of order  $\phi_d$  and Glandt equation gives the same results as Maxwell model. In other words, comparison of the Maxwell and the Glandt model indicates that, although the particle size was neglected in the Maxwell equation compared with the mean distance within the particles, the interaction between the particles and the continuous media is considered.

## 2.1.4 Effects of Environmental Conditions on Polymer Permeability

### 2.1.4.1 *Temperature Effects on Permeability*

The thermal effects on solubility and diffusion show opposite trends. Generally, for gas adsorption, solubility decreases with increases in temperature due to the condensability of the penetrant at lower temperatures. The solubility dependence with temperature is typically written in terms of the Van't Hoff relationship shown in Eq. (2.15).

$$S = S_o \cdot \exp\left(-\frac{\Delta H_s}{R \cdot T}\right) \quad (2.15)$$

where  $S_o$  is a constant and  $\Delta H_s$  is the partial molar enthalpy of sorption.

The solubility in thermodynamic terms is a two steps process. The first step involves the condensation of the gas molecule in a polymer, followed by creation of a molecular scale gap for accommodating the gas molecule. These individual steps contribute to the total enthalpy of sorption and are mathematically represented as:

$$\Delta H_s = \Delta H_{condensation} + \Delta H_{mixing} \quad (2.16)$$

For low molecular weight super critical gases, low condensability causes the mixing step to control the sorption property of a polymer. For weak interactions between the gas molecule and the polymer, the change in enthalpy of mixing is positive. This leads to an increase in solubility with an increase in temperature. For the case of condensable gases and vapors, the enthalpy change for condensation is negative and dominant, thereby showing decreasing solubility with increasing temperature.

Whereas the temperature dependence on gas diffusion is expressed in terms of an Arrhenius type relationship, as movement of gas molecules through a membrane is considered a thermally activated process. Mathematically, the temperature dependence of diffusion is given as:

$$D = D_o \cdot \exp\left(\frac{\Delta E_D}{R \cdot T}\right) \quad (2.17)$$

where  $D_o$  is the pre exponential factor and  $E_D$  is the activation energy of diffusion.

Studies on the thermal effects during gas transport have shown that the activation energy term is dependent on the size of the penetrant and not on its mass. Diffusion is the most temperature sensitive transport parameter, in comparison to solubility and permeability. Combining the temperature dependence equations for the diffusion and sorption coefficients, the temperature effect on gas permeability is given as:

$$P = P_o \cdot \exp\left(\frac{\Delta E_p}{R \cdot T}\right) \quad (2.18)$$

where  $E_p$  is the activation energy of permeation and is an algebraic sum of  $E_D$  and  $\Delta H_s$ .

In general, permeability increases with increasing temperature. However, there are exceptions, especially near the glass transition temperature of the polymer, where opposite trends have been observed. These observations were explained in terms of pressure effects on the polymer under isothermal operating conditions. The high stress caused by the applied gas pressure was stated to cause a transition in the polymer from a rubbery state to a glassy state.

#### 2.1.4.2 Pressure and Concentration Effects on Permeability

The effects of pressure and the gas concentration in the membrane are a major challenge in effective modeling of the gas transport process. Typical effects of gas pressure on permeability are shown in Figure 2.3.

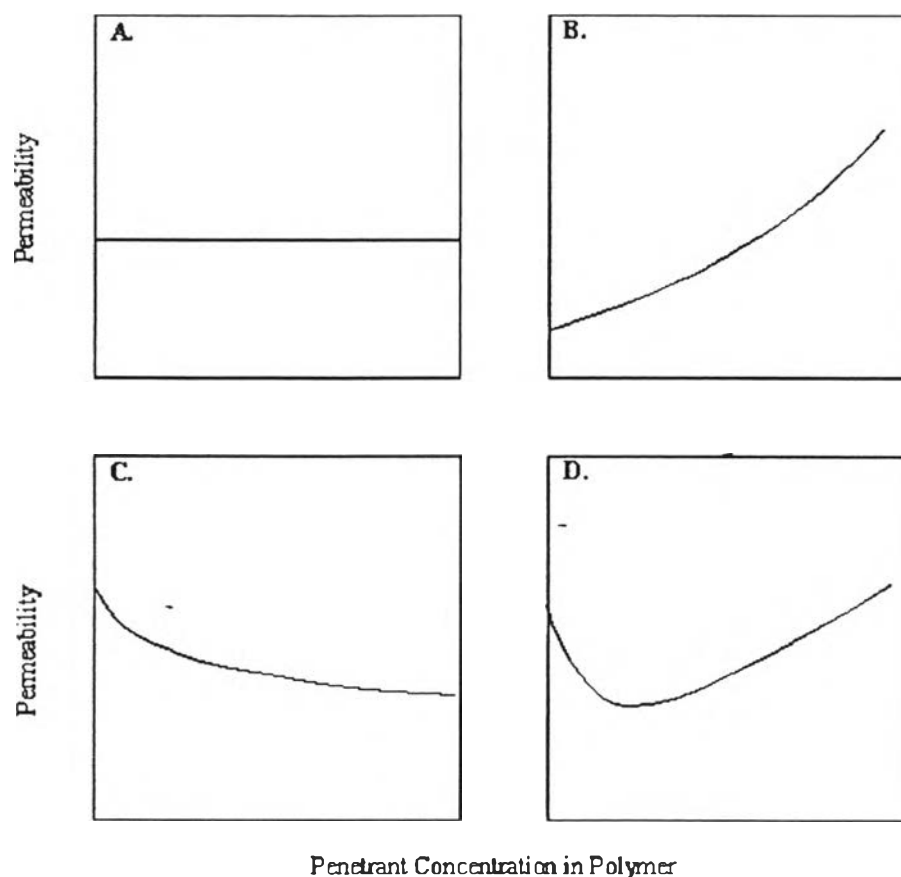


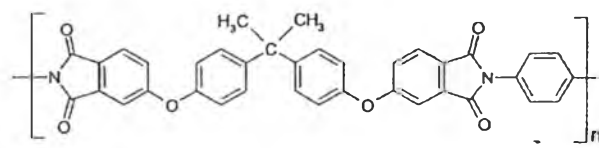
**Figure 2.3** Typical forms of permeability dependence on gas concentration during gas transport through polymer membranes (Koros *et al.*, 1987).

The first response (response A) is for the ideal case as both diffusion and solubility are assumed independent of gas pressure. This type of behavior is observed for the case of supercritical gas permeation in amorphous polymers. The response B is characteristic of a gas plasticization effect on the polymer and is observed during organic vapor permeation in rubbery polymers. Response C corresponds to the case of highly soluble gases in glassy polymer. The last response (D) is a combination of the responses (B) and (C) and is observed in the case of permeation of organic vapors or plasticizing gas, such as  $\text{CO}_2$ , in glassy polymers.

### 2.1.5 Ultem Polymer and Metal-Organic Framework Properties

Ultem polymer and two types of MOF used in this work are commercial products. The product information of Ultem and MOFs is obtained from SABIC Innovative Plastics Co., Ltd. and Singma Aldrich Co., Ltd., respectively.

**Table 2.1** Chemical structure and physical properties of Ultem<sup>®</sup>1000 (www.sabic-ip.com)

Polymer	Chemical Structure	Density (g/cm <sup>3</sup> )	T <sub>g</sub> (°C)
Ultem <sup>®</sup> 1000		1.27	215

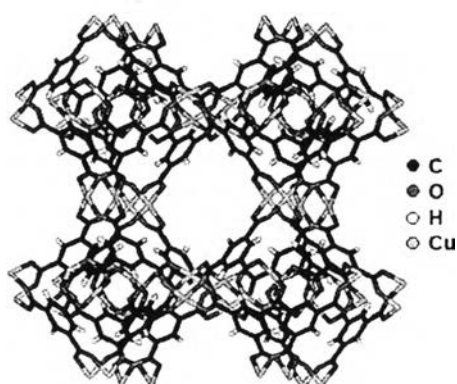
Ultem is a high-strength amorphous polymer with excellent heat as well as flame resistance with little smoke output, making it superior to other polymers such as polysulfone. The standard color of Ultem is amber. The chemical structure and physical properties of Ultem polymer are displayed in Table 2.1. The aromatic imide units provide stiffness and heat resistance, while the swivel groups such as  $-O$  and  $-C(CH_3)_2$  form flexible macromolecular chains that allow for good processability (Kurdi and Tremblay, 1998). Ultem is an engineering polymer with high selectivity for  $CO_2/CH_4$  with considerable flexibility provided by the ether linkage in the polymer backbone. Moreover, Ultem polymer has high glass transition temperature ( $T_g = 215^\circ C$ ) which provides more resistant to stresses and poses greater challenges as a mixed matrix material (Vu *et al.*, 2003).

Physical properties of MOF-199 and ZIF-8 are shown in Table 2.2, as well as the chemical structures and SEM images of MOF-199 particles and ZIF-8 particles are shown in Figures 2.4 and 2.5, respectively.

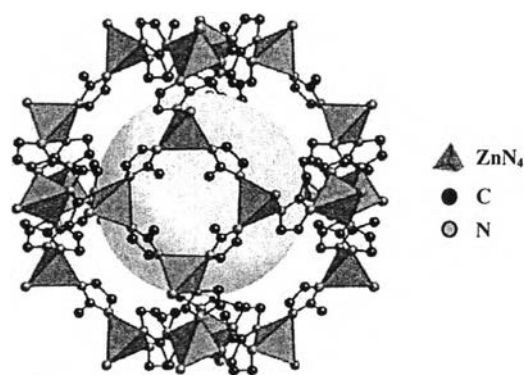
**Table 2.2** Physical properties of MOF-199 and ZIF-8

(http://www.sigmaaldrich.com/catalog/product)

MOFs	BET surface area (m <sup>2</sup> /g)	Particle size (D50, μm)	Density (g/cm <sup>3</sup> )
MOF-199	1500-2100	15.96	0.35
ZIF-8	1300-1800	4.9	0.35



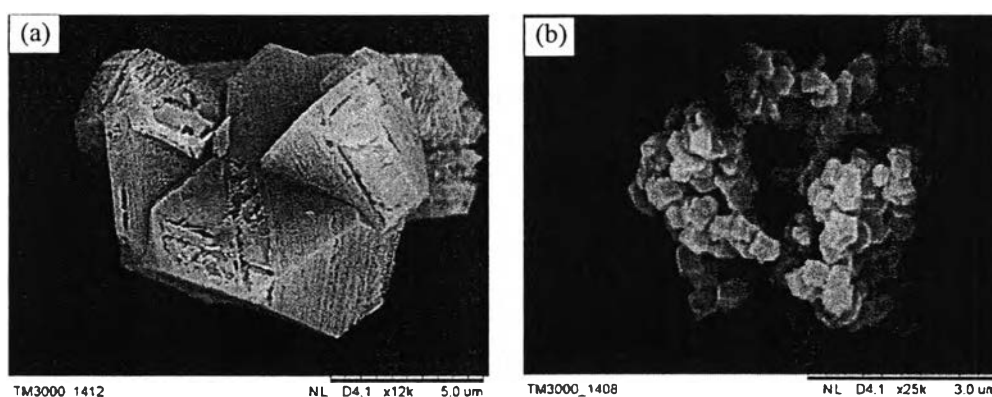
(b) MOF-199



(a) ZIF-8

**Figure 2.4** The chemical crystal structures of MOF-199 and ZIF-8

(Yang and Zong, 2006).

**Figure 2.5** SEM images of metal organic frameworks; (a) MOF-199 and (b) ZIF-8.

MOF-199 ( $\text{Cu}_3(\text{BTC})_2$ , Cu with BTC = benzene-1,3,5-tricarboxylate), also known as HKUST-1, is one of the most widely studied MOFs. Its chemical structure is displayed in Figure 2.4 (a). MOF-199 has a very high BET surface area (1500-2100 m<sup>2</sup>/g) with metal corners consisting of  $\text{Cu}^{2+}$  ions coordinated to 1,3,5-

benzenetricarboxylate organic linkers. A distinct cubic crystalline structure and particle size of around 6  $\mu\text{m}$  was observed from Figure 2.5 (a). It has main channels 9  $\text{\AA}$  in diameter surrounded by tetrahedral pockets of 5  $\text{\AA}$  in diameter. The tetrahedral pockets and the main channels are connected by triangular windows of diameter 3.5  $\text{\AA}$ .

Zeolitic imidazolate frameworks (ZIFs) are a class of MOFs with tetrahedral networks that resemble structure types of conventional zeolites. ZIF-8 crystallizes in the sodalite topology (SOD) and consists of Zn(II) tetrahedrally coordinated by four 2-methylimidazolate linkers as shown in Figure 2.4 (b). The rate-limiting step for the diffusion of guest molecules is the passage through the six-membered windows connecting each cavity. The window size is estimated to be 3.4  $\text{\AA}$  by X-ray diffraction structure analysis (Dai *et al.*, 2012).

## 2.2 LITERATURE REVIEW

Conventional membranes used for gas separation are classified as inorganic membranes, polymeric membranes, and mixed matrix membranes. With each type of the membranes used, further classification is based on the materials of membranes.

### 2.2.1 Inorganic Membranes

Inorganic membranes like ceramic membranes of metal oxides ( $\gamma\text{-Al}_2\text{O}_3$ ,  $\text{ZrO}_2$ ,  $\text{TiO}_2$  or  $\text{ZrTiO}_4$ ), zeolites, porous carbon membranes, metal membranes or porous glass membranes are useful for  $\text{CO}_2$  separation under severe conditions (high temperature and pressure). These membranes can be categorized into porous and non-porous types. Porous inorganic membranes such as zeolites, which contain sub-nanometer pores, are favorable for  $\text{CO}_2$  separation and removal from  $\text{CH}_4$  because of their chemical resistance to  $\text{CO}_2$  induced plasticization and superior selectivity to polymeric membranes. Zeolites membranes normally consist of polycrystalline films of aluminosilicates loaded on porous supports.

Other porous inorganic membranes such as silica and carbonized membranes are also available but less popular than zeolites. Both membranes normally separate  $\text{CO}_2$  from other gases including  $\text{CH}_4$  by molecular sieving

principles e.g. silica has subnanometer sized pores which would pass different gases according to their sizes.

Hassan *et al.* (1995) investigated the gas separation properties of silica hollow fiber membranes with pore size ranging between 5.9 Å and 8.5 Å. They conducted both single and mixed gas experiments using light gases and hydrocarbons with kinetic diameters ranging from 2.6 to 3.9 Å. They observed large separation factors for carbon dioxide/methane mixtures, which was attributed to surface diffusion as being the primary transport mechanism. The mixed gas selectivity was higher than single gas, which they concluded was due to the competitive adsorption effects.

Inorganic membranes typically have the advantage of higher permeabilities as compared to polymeric membranes, and selectivities are high when certain transport mechanisms are dominant. Inorganic membranes also exhibit good resistance to harsh chemical conditions and can withstand high pressures and temperatures. However, one major drawback of inorganic membranes is that selectivity tends to be a strong function of process conditions, especially temperature, pressure and mole fraction of the condensable species in the feed.

### 2.2.2 Polymeric Membranes

Gas separation using polymeric membrane has achieved important success as high separation performance membrane since the first commercial scale membrane gas separation system which was produced in the late 1970s. There are two types of polymeric membrane used for gas separation. Firstly, glassy polymeric membranes are rigid and operate below their glass transition temperature ( $T_g$ ). Secondly, rubbery polymeric membranes are flexible and operate above their glass transition temperature. Polymeric membranes are still ineffective in meeting the requirement for the current advanced membrane technology as these materials have demonstrated a trade-off between the permeability and selectivity, with an 'upper-bound' evident as proposed by Robeson (Goh *et al.*, 2011). A correlation of membrane separation data offering an analysis of the limits of polymer permeability and selectivity is often referred to as the upper boundary in which the gas separation properties of the polymeric membranes follow distinct trade-off relations where more



permeable polymers are generally less selective and vice versa. The revisited upper bound relationship by Robeson for CO<sub>2</sub>/CH<sub>4</sub> membrane separation for polymeric membranes is illustrated in Figure 2.6.

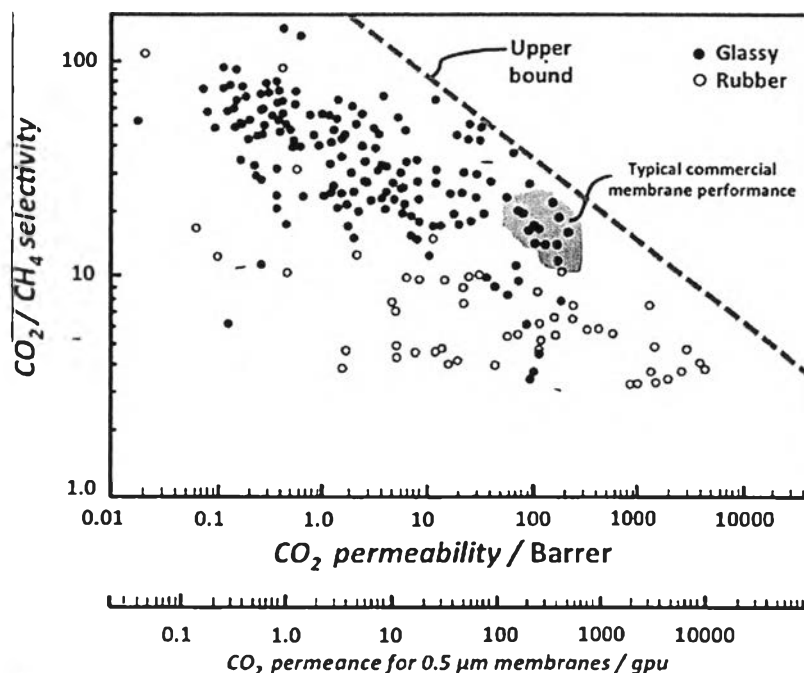


**Figure 2.6** Robeson plot for the separation of CO<sub>2</sub> from CH<sub>4</sub> (Zornoza *et al.*, 2013).

This represents the selectivity obtained from the ratio of pure gas permeability plotted against carbon dioxide permeability for different polymeric membranes. A permeance of 1 GPU corresponds to a membrane exhibiting an intrinsic permeability of 1 Barrer and having a selective layer thickness of 1 μm.

However, glassy polymeric membranes dominate industrial membrane separations because of their higher gas selectivity, in addition to better mechanical properties compared to that of rubbery polymers. Thus, this section will focus on literatures which involve glassy polymeric membrane only.

### 2.2.3 Mixed Matrix Membranes (MMMs)

To enhance the commercial applicability of polymer membrane separation process, Kulprathipanja and coworkers at UOP LLC (1986 and 1988) developed the MMM that allows the membrane selectivity to be increased through gas solubility optimization. MMMs consist of a continuous phase (polymer) and a

homogeneously distributed discrete phase (typically inorganic particles). The purpose of including inorganic particles is to increase the property of polymer matrix. Over the past decades, several types of fillers have been explored in order to establish MMM with higher gas separation performance.

#### 2.2.3.1 Zeolite

For the last few decades, the improvement in MMM performance using zeolite as the dispersed phase has resulted in the commercial alternative over the polymeric and inorganic membrane. The use of zeolite in the formation of MMM as potential filler for gas separation membranes has received numerous attentions due to their thermal stability as well as their promising separation and transport properties. Shape selectivity and specific sorption characteristics of zeolite can be combined with easy processability of polymer to provide desired properties in zeolite filled MMM. Numerous numbers of reports have indicated the favorable effects of employing zeolite as the dispersed phase to improve the permeability and selectivity of various polymers for gas separation of different gas pairs (Goh *et al.*, 2011).

SAPO-34 zeolite has 0.38 nm pores and is studied for membrane separation of CO<sub>2</sub> from natural gas feeds (Li *et al.*, 2006). These mixtures are available at pressures of 7.2 MPa with CO<sub>2</sub> concentrations of up to 50% and temperatures up to 50°C. The SAPO structure remains unsaturated for CO<sub>2</sub> at those conditions so that it is highly permeable and selective for CO<sub>2</sub>. However, the authors mentioned that this type of zeolite did not economically for the industrial scale due to high synthesis cost.

Zeolite Y contains 1.3 nm pore super cages, connected by 0.73 nm windows in a tetrahedral arrangement. Zeolite Y membranes have been studied in the past 10 years for their special CO<sub>2</sub> selectivity at ambient pressures and temperatures. Recently it was found that Zeolite Y membrane on high-quality supports have a CO<sub>2</sub>/N<sub>2</sub> selectivities of well over 100 for temperatures up to 80°C and CO<sub>2</sub> partial pressures of more than 15 kPa (White *et al.*, 2010). This makes Zeolite Y attractive for capture of CO<sub>2</sub> from flue gas.

On the other hand, zeolites particle face the problem of formation of aggregates creating defects, especially if the polymer matrix is

consisting of a glassy polymer. Poor adhesion at the zeolite-polymer interface can result in “sieve-in-a-cage” morphology that is responsible for the nonselective penetration of gas molecules, hence reduce the apparent selectivity of the mixed matrix membrane and increase the permeability. Several attempts of modifying the surface of the zeolites to chemically bond them to the polymer chains and avoid macro-void formation have been made, which often led to a considerable decrease of the gas permeability due to the rigidification of the polymer chains near the zeolite surface. Surface modification of zeolite using silanes that enables chemical link between zeolite particles and the polymer matrix is also proven to be an effective approach to improve both interfacial adhesion and gas selectivity of the MMM by modifying the surface properties of zeolite from hydrophilic to hydrophobic as well as increasing zeolite affinity to the functional groups of the polymer matrix (Verweij, 2012).

#### 2.2.3.2 Carbon Molecular Sieve (CMS)

In 2003, Vu *et al.*'s experimental work is an ideal case to describe the aforementioned effect. They investigated the effect of CMS 800-2 (as porous inorganic filler) on the separation properties of Matrimide 5218 and Ultem 1000 (as polymer matrices). They showed that with addition of 36 vol% CMS 800-2 (with CO<sub>2</sub> permeability 44 Barrer and CO<sub>2</sub>/CH<sub>4</sub> selectivity 200) into the Matrimide matrix (with CO<sub>2</sub> permeability 10 Barrer and CO<sub>2</sub>/CH<sub>4</sub> selectivity 35.3), the CO<sub>2</sub> permeability of resulting MMM increases from 10 Barrer to 12.6 Barrer and the CO<sub>2</sub>/CH<sub>4</sub> selectivity increases from 35.3 to 51.7. They also found a similar effect for addition of 35 vol% CMS to Ultem (e.g. an increase in CO<sub>2</sub> permeability from 1.45 to 4.48 Barrer and an increase in the CO<sub>2</sub>/CH<sub>4</sub> selectivity from 38.8 to 53.7). Figure 2.7 compares the separation property of CMS, neat Ultem and Matrimide membranes and CMS-Ultem and CMS-Matrimide mixed matrix membranes.

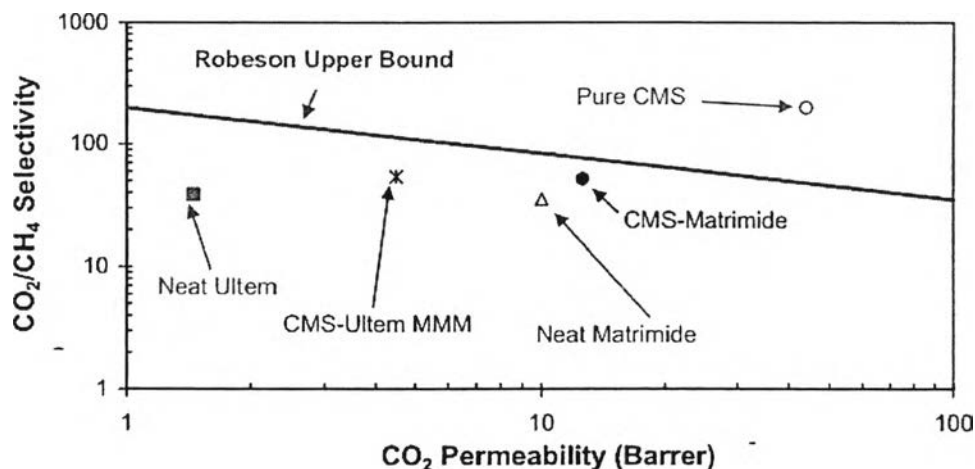


**Figure 2.7** Effect of CMS on the performance of polymeric Matrimide and Ultem membranes (Vu *et al.*, 2003).

As shown in Figure 2.7, CMS as a porous dispersed phase can increase separation properties of both polymeric Ultem and Matrimide polymeric membranes close to the known Robeson upper bound.

Activated carbon is a good example of large pore size inorganic fillers. Anson *et al.* (2004) used two kinds of activated carbon for MMM fabrication using acrylonitrile–butadiene–styrene copolymer (ABS) as the polymer matrix. They reported the mean pore sizes of used activated carbons, called AC1 and AC2, as 21.7 Å and 28.2 Å, respectively. It is obvious that the pore sizes of the activated carbons used as the porous inorganic fillers are bigger than the molecular diameter of CO<sub>2</sub> and CH<sub>4</sub> which were used as test gases. This means that the used activated carbons cannot separate the gas molecules (e.g. CO<sub>2</sub> and CH<sub>4</sub>) by the sieving mechanism and so the surface flow mechanism should be considered. In other words, adsorbability of penetrants is a key separation character of activated carbons and should be taken into account when they are used as fillers in the polymer matrix. Anson *et al.* measured adsorption properties of used activated carbons for each gas at temperatures between 293 K and 323 K and equilibrium pressures of 2–8 bar and showed that both activated carbons have a higher adsorption selectivity for CO<sub>2</sub> (more adsorbable gas) than for CH<sub>4</sub> (less adsorbable gas). For example AC1 was 3–3.5 times more selective for CO<sub>2</sub> adsorption than CH<sub>4</sub> whereas adsorption selectivity of the AC2 was 1.6–2.7 for CO<sub>2</sub> over the CH<sub>4</sub>. These large pore size

fillers embedded into the ABS polymer matrix could increase the  $\text{CO}_2/\text{CH}_4$  selectivity of resulting MMM by 1.45–2.1 times that of the neat ABS membrane. As it has been described earlier, the authors attributed this phenomenon to surface diffusion of more adsorbable gas penetrant ( $\text{CO}_2$ ) over the less adsorbable component ( $\text{CH}_4$ ) through the micro-mesoporous activated carbons in the polymer matrix.

### 2.2.3.3 Metal Organic Frameworks (MOFs)

The first MOF–MMM comprised a three dimensional copper (II) biphenyl dicarboxylate–triethylenediamine MOF embedded in PAET (poly(3-acetoxyethylthio phen)) for gas separation. The resulting composite displayed an enhanced  $\text{CH}_4$  permeability at 20 wt% and 30 wt% of MOF loading. The authors claimed that the increase in hydrophobicity of the MMMs might preferentially increase the adsorption of methane in the copper MOF, resulting in an increase in permeability. However, a decrease in  $\text{CO}_2$  permeability, and therefore a reduction of the  $\text{CO}_2/\text{CH}_4$  was observed (Yehia *et al.*, 2004). Since this pioneering work, the interest in MOF–MMMs has been growing and it has already been demonstrated that, by choosing the proper MOF-polymer couple, it is possible to surpass the Robeson's upper bound for several important separations.

Mahajan *et al.*, (2004) reported an MMM comprised of poly(vinyl acetate) (PVAc) and a MOF composed of copper and terephthalic acid (Cu–TPA). This membrane exhibited increased selectivity for many gases, including  $\text{CO}_2$  upon inclusion of the MOF compared to the pure PVAc membrane. The ideal selectivity of pure PVAc for  $\text{CO}_2/\text{N}_2$  is 32 and for 15% CuTPA–PVAc is 35. All gases were tested at 65 psia (4 atm) except for  $\text{CO}_2$  which was tested at 1.35 psia (0.09 atm) to prevent plasticization.

Zhang *et al.* (2008) explored the same trend with Cu–BPY–HFS (Cu-4,4' bipyridine-hexafluorosilicate) MOF. In this case, the polyimide Matrimid<sup>®</sup> was the chosen polymer to study the pure gas permeation of  $\text{H}_2$ ,  $\text{N}_2$ ,  $\text{O}_2$ ,  $\text{CH}_4$  and  $\text{CO}_2$ , as well as the separations of  $\text{CO}_2/\text{CH}_4$ ,  $\text{H}_2/\text{CO}_2$  and  $\text{CH}_4/\text{N}_2$  mixtures. An increase in solubility and hence of selectivity was only found towards  $\text{CH}_4$  ( $\text{CH}_4/\text{N}_2$  separation factor from 0.95 to 1.7 with 20 wt% of MOF) attributed to the high hydrophobicity of the MOF.

The first patent on MOF MMMs dealt with the use of IRMOF-1 (Liu *et al.*, 2009). Up to 20 wt% of IRMOF-1 particles were dispersed in Matrimid<sup>®</sup> polyimide and Ultem<sup>®</sup> polyetherimide. Single gas permeation measurements showed the improvements in CO<sub>2</sub> and H<sub>2</sub> gas permeabilities compared to the pure polymers without significant decrease in the corresponding ideal selectivities.

In the same line, Perez *et al.* (2009) reported an increase in permeability with almost constant ideal selectivity from the neat polymer (Matrimid<sup>®</sup>) to the 30 wt% of MOF-5 loading for H<sub>2</sub>, CO<sub>2</sub>, O<sub>2</sub>, N<sub>2</sub> and CH<sub>4</sub>. At that loading, CO<sub>2</sub> permeability showed an increase of 55%, CH<sub>4</sub> did 100%, while the CO<sub>2</sub>/CH<sub>4</sub> separation factor increased by 6%. Matrimid<sup>®</sup> incorporated with MOF-5 has exhibited a remarkable increase in selectivity for CH<sub>4</sub> due to the coupling effect of favorable MOF-5 affinity towards CH<sub>4</sub> and larger solubility of CO<sub>2</sub> and N<sub>2</sub>.

A molecular simulation study of gas mixtures permeating through MMMs containing IRMOF-1 in Matrimid<sup>®</sup> was performed by Keskin and Sholl (2010). The authors described the predicted performance of Cu(hfipbb) (H<sub>2</sub>hfipbb)<sub>0.5</sub> MMMs using Maxwell and Bruggeman models. They illustrated that 20 wt% Cu(hfipbb) (H<sub>2</sub>hfipbb)<sub>0.5</sub> was enough to bring the MMM above the Robeson's upper bound with a CO<sub>2</sub>/CH<sub>4</sub> selectivity of 72 and CO<sub>2</sub> permeability of 15.7 Barrer.

Adams *et al.* (2010) synthesized a MOF of copper and terephthalic acid (CuTPA) incorporated into poly(vinyl acetate) (PVAc) matrix for making MMM. The results showed that pure gas permeabilities and selectivities of 15% CuTPA–PVAc MMMs showed improvements over pure PVAc properties.

Recently, a new class of MOF with exceptional chemical stability, zeolitic imidazolate framework (ZIF) with tetrahedral network and sodalite cagelike structure that resemble the structure type of zeolite has been identified as an attractive molecular sieve for small gas molecules such as H<sub>2</sub> and CO<sub>2</sub> (Goh *et al.*, 2011).

Ordenez *et al.* (2010) reported the first ZIF-based polymer MMM using ZIF-8 as the filler phase and Matrimid<sup>®</sup> as the polymer phase. Inclusion of the ZIF phase had substantial impact on the membrane selectivity. Pure Matrimid<sup>®</sup>

exhibited an ideal selectivity for CO<sub>2</sub>/CH<sub>4</sub> of 43, and at 50% loading of ZIF crystals the ideal selectivity increased to 124. Binary gas measurements of 10:90 CO<sub>2</sub>/CH<sub>4</sub> also showed selectivity enhancement; pure Matrimid<sup>®</sup> gave selectivity of 42, and at 50% loading the selectivity increased to 89.

Bae *et al.* (2010) have reported the performance of ZIF-90/6FDA-DAM MMM that surpassed the trade-off of polymeric membrane performance in which the enhancement in both permeability and selectivity was mainly due to the selective sorption and diffusion of CO<sub>2</sub> in the ZIF-90 crystal.

Ordóñez *et al.* (2010) using ZIF-8/Matrimid<sup>®</sup> MMM, significant increase in the gas permeability was observed at ZIF-8 loading lower than 50 w/w% due to the presence of MOF fillers that has increased the distance between polymer chains and disrupted chain packing in the polymer thus showing an increase in the free volume. A remarkably enhanced selectivity for gas pairs containing small gas molecules was reported at 50% ZIF loading. The increment of 213% and 290% for CO<sub>2</sub>/CH<sub>4</sub> and H<sub>2</sub>/CH<sub>4</sub> selectivity, respectively, was ascribed to the molecular sieving effect of the small pore aperture of ZIF-8 that favors the diffusion of small gas while hindering the easy diffusion of large gas molecules like CH<sub>4</sub>.

Basu *et al.* (2011) obtained both an increase in carbon dioxide permeance and CO<sub>2</sub>/CH<sub>4</sub> selectivity by combining the commercial MOFs Cu<sub>3</sub>BTC<sub>2</sub>, ZIF-8 and MIL-53 with Matrimid<sup>®</sup>. The effects were less pronounced with addition of ZIF-8 (Zn) and MIL-53 (Al). Also changing to CO<sub>2</sub>/N<sub>2</sub> separation showed less significant improvements. Moreover, Dai *et al.* (2012) found a significant increase in carbon dioxide permeance and a 20% enhanced carbon dioxide/nitrogen selectivity when ZIF-8 was combined with Ultem<sup>®</sup> as polymer matrix.

As mentioned above, ZIFs facilitate the transport of small molecules through the aperture and into the pore, competitive adsorption for gas pair contains both small molecules cannot be realized by these ZIFs.

Liu *et al.* (2009) in their patent reported the fabrication of 30 wt% MOF-199/Matrimid MMMs. Their results showed an increase in CO<sub>2</sub> permeability without any loss of CO<sub>2</sub>/CH<sub>4</sub> selectivity compared to a neat Matrimid membrane. In another work, Basu *et al.* (2010) synthesized MOF-199/Matrimid and MOF-199/Matrimid-polysulphone blends MMMs via the phase inversion method.

Their results showed that  $\text{CO}_2/\text{CH}_4$  selectivity increased with filler loading depending on  $\text{CO}_2$  concentration at 10 bar and  $35^\circ\text{C}$ . Also the  $\text{CO}_2$  permeability of MMMs increased upon adding the filler.

Recently, Hu *et al.* (2010) synthesized hollow fibers of MOF-199/ polyimide MMMs for gas separation and adsorption. However, their results showed a reduction in  $\text{CO}_2$  permeation without any change in  $\text{CO}_2/\text{CH}_4$  selectivity at both the 3 and 6 wt% filler loadings compared to the neat polymeric membrane.

Car *et al.* (2011) used MOF-199 with two polymer matrices, poly-dimethylsiloxane (PDMS) and polysulfone (PSf) to make MMMs for gas separation. Their results showed an increase in permeability of  $\text{CO}_2$  without any changes in the  $\text{CO}_2/\text{CH}_4$  selectivity in PDMS-based MMMs compared to a neat polymer membrane. Both the  $\text{CO}_2$  permeability and  $\text{CO}_2/\text{CH}_4$  selectivity increased in PSf-based MMMs at 5 wt% filler loading. By increasing the filler loading to 10 wt%, the selectivity decreased significantly. The authors described this effect occurred from the presence of voids at the interface of MOF particles and polymers due to the agglomeration of the fillers.